High Gain Circularly Polarized X-shaped Aperture Coupled Antenna for WLAN Applications

Mohammed A. Meriche [1,2], Abderraouf Messai [1], Tayeb A. Denidni [2], and Hussein Attia [3]

[1] Department of Electronics
Université des frères Mentouri, Constantine, Algeria

[2] EMT-INRS, Institut National de la Recherche Scientifique
800, rue De La Gauchetière O, Montréal (Qc) H5A 1K6 Canada

[3] King Fahd University of Petroleum and Minerals (KFUPM)
Dhahran 31261, Saudi Arabia

Abstract — This paper presents a new high gain compact aperture-coupled circularly polarized antenna for WLAN applications. The proposed antenna comprises an asymmetric X-shaped slot etched on a circular patch and fed through the coupling between an annular slot and a microstrip line. The circular polarization is mainly due to the asymmetrical crossed-slots, respecting the angle of 45^0 between its two arms. The antenna with overall size of $60 \times 60 \times 5.83$ mm^3 has a measured 10-dB impedance bandwidth of 36%, a 3-dB axial ratio bandwidth of 3.47% (5.67–5.87 GHz) and 1-dB gain bandwidth of 19.5% (4.85-5.90 GHz) with a peak gain of 8.65 dBi. To validate the simulated results, a prototype was fabricated, and good agreement between simulations and measurements has been accomplished.

Index Terms — Aperture-coupled, axial ratio, circularly polarized (CP), X-shaped slot.

I. INTRODUCTION

Recently, high gain antennas have been widely used for WLAN applications. To realize this type of antennas, different techniques are used in literature. These techniques include the integration of electromagnetic band gap (EBG) structures in ground plane acting as artificial magnetic conductor [1-2] or superstrates acting as partially reflective selective surface [3-5]. In this work, the aperture-coupled antenna method is used to enhance the antenna gain without using any EBG structures.

Circularly polarized (CP) patch antennas have attracted substantial attention in modern wireless communication systems due to its many advantages such as more flexibility in the orientation of transmitting and receiving antennas and polarization mismatch reduction compared to linear polarization [6-10].

The most popular types of single-fed CP patch antennas are the slotted and the notched patch [11-16]. Several methods have been proposed to design single-feed aperture-coupled antennas with CP [17-21]. The aperture-coupled antennas were designed and developed for broadband, high gain, CP and high efficiency applications. Therefore, single-fed aperture-coupled antennas with CP characteristics have received greater attention [17-20] over the past decade.

In this paper, a novel compact aperture-coupled CP antenna for WLAN applications is proposed. The new antenna consists of an asymmetric X-shaped slot with an angle $\theta = 45°$ between its two arms, the slotted antenna is etched on a circular patch fed through the coupling between an annular slot and a microstrip line. The CP is generated by cutting two unequal slots in the circular patch respecting the angle θ. This paper is organized as follows. In Section 2, the design of the proposed antenna is described. Section 3 presents fabrication and measured results. Finally, concluding remarks are given in the last Section.

II. ANTENNA DESIGN

The proposed configurations of the CP antenna fed through a microstrip-coupled annular slot is shown in Fig. 1. The X-shaped slot with unequal arms, width W_s, lengths L_1 and L_2 etched on a circular patch and the annular slot aperture feeding are depicted in the Figs. 1 (b) and 1 (c).

The annular slot with outer radius R_o and inner radius R_i with the microstrip feed line are etched on a Rogers RO4003C substrate of thickness h_1, relative permittivity of 3.38, and loss tangent $\tan\delta = 0.0027$. The 50-Ω microstrip feed line with length L_f and width W_f is printed at the center of the bottom side of the ground plane and is electromagnetically coupling the energy to the annular slot. Moreover, the aperture feed is employed to directly excite the X-shaped slot on the circular patch. An optimum air gap height of H_c between the X-shaped

Submitted On: January 14, 2018
Accepted On: August 17, 2019

slot antenna substrate and aperture-coupled substrate is employed. The aperture-coupled substrate of Rogers RO4003C is identical to the one employed for the X-shaped slot circular patch.

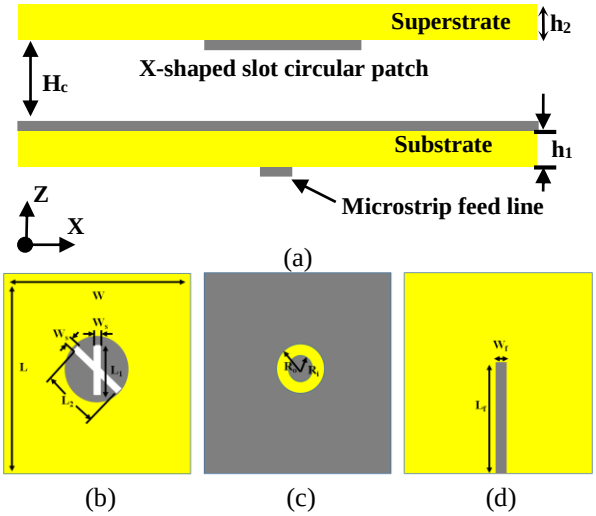

Fig. 1. Geometry of the proposed antenna: (a) side view, (b) bottom view of the X-shaped slot circular patch, (c) top view of the annular slot aperture coupling ground, and (d) the microstrip feed line.

The proposed antenna was simulated using the commercial software package CST Studio Suite. CST comprises three different solvers. These solvers are transient (i.e., time domain) solver based on finite integration technique (FIT), frequency domain solver based on finite element method (FEM), and integral equation solver based on method of moments (MoM). The transient solver has been adopted in this work due to its computational and memory-efficient performance. FIT is a finite difference method based on a small-scale interpretation of Maxwell's equations (as opposed to a large-scale integral equation approach). The formulation of the FIT utilizes voltage and current (i.e., integral of E and H fields), on a staggered grid.

Table 1: The detailed dimensions of the proposed antenna (all dimensions are in mm)

Parameter	Value	Parameter	Value
W	60	h_1	1.524
L	60	h_2	0.81
L_1	15	H_c	3.5
L_2	17	R_i	5
W_s	2	R_o	7
L_f	30	R (circular patch radius)	9.5
W_f	3.55		

Parametric sweep tool in CST is utilized to carefully choose the feed location, the annular slot and the X-shaped slot dimensions in order to obtain good impedance matching and CP. These dimensions have been swept within certain boundaries (about ± 25% of the selected value) to enable the calculation of far-fields or impedances based on the swept parameters. Table 1 presents the selected parametrized dimensions of the compact aperture-coupled CP antenna demonstrated in Fig. 1.

The performance of the proposed CP antenna is studied in order to gain a better insight into the effects of the X-shaped slot antenna over the whole structure and how the CP radiation is obtained. Figure 2 depicts the geometry of the X-shaped slot etched on the circular patch with different values of the angle θ between the asymmetrical crossed-slots of lengths L_1 and L_2. The variation of the angle θ may affect the impedance bandwidth and the CP behavior. Figures 3 and 4 show the parametric studies of the reflection coefficient (S_{11}) and the axial ratio (AR) versus the angle θ.

The angle θ is varied from 0° to 90° while L_1, L_2 are fixed (L_1 = 15 mm, L_2 = 17 mm). Only when θ = 45° the impedance matching gets better and covers the WLAN band as shown in Fig. 3.

Figure 4 shows the variation of AR at broadside. The AR improves when the angle θ = 45°, for θ = 0° and θ = 90° it can be seen that the minimum AR is about 40 dB, which implies that no circular polarisation has been achieved.

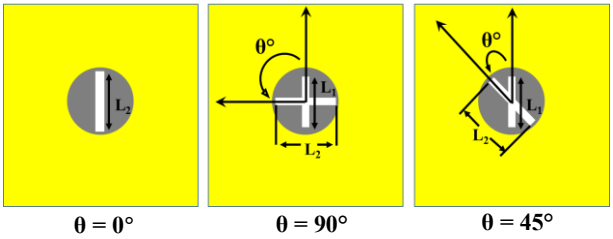

Fig. 2. Geometry of the asymmetrical crossed-slots etched on the circular patch with variation of theta.

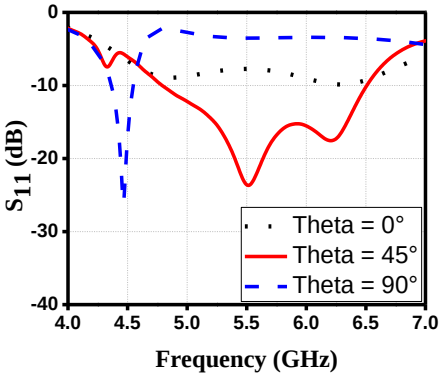

Fig. 3. Simulated reflection coefficient of the antenna with variation of the angle theta.

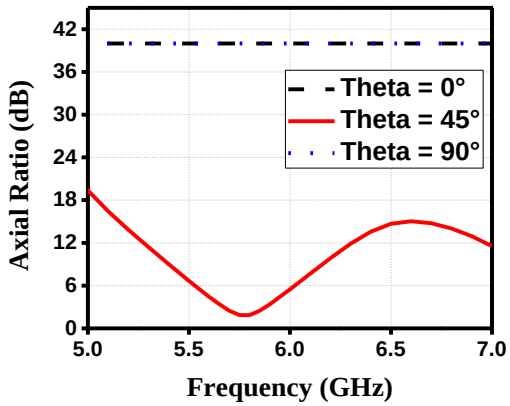

Fig. 4. Simulated axial ratio of the antenna with variation of the angle theta.

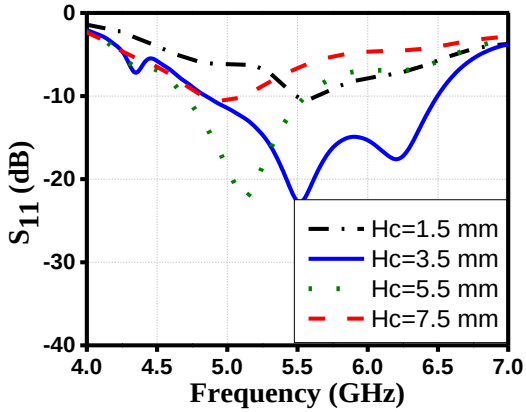

Fig. 5. Simulated reflection coefficient of the antenna with variation of H_c.

The distance between the feeding annular slot and the X-shaped slot is expected to affect the impedance bandwidth. Figure 5 shows the parametric studies of the reflection coefficient (S_{11}) versus the distance H_c. H_c is varied from 1.5 to 7.5 mm and L_1, L_2 are fixed (L_1 = 15 mm, L_2 = 17 mm). When H_c is increased from 1.5 to 3.5 mm, the impedance matching gets even better, then when the distance H_c is increased from 5.5 to 7.5 mm the impedance matching bandwidth shifts down.

Figures 6 and 7 show the parametric analysis of the reflection coefficient and the AR versus the lengths of asymmetrical crossed-slots L_1 and L_2. Within the operating frequency band and with an optimum gap height of H_c = 3.5 mm, only one geometrical parameter (L_2) is varied each time and the second parameter (L_1) is kept unchanged. Figure 6 presents the variation of reflection coefficient with $L_1>L_2$, $L_1=L_2$ and $L_1<L_2$. The S_{11} bandwidth improves as $L_1<L_2$ and the impedance matching also improves and gets even better, with an impedance bandwidth of 1.7 GHz (from 4.8 GHz to 6.5 GHz) which is about 30%. Figure 7 shows the variation of AR at broadside, with $L_1>L_2$, $L_1=L_2$ and $L_1<L_2$.

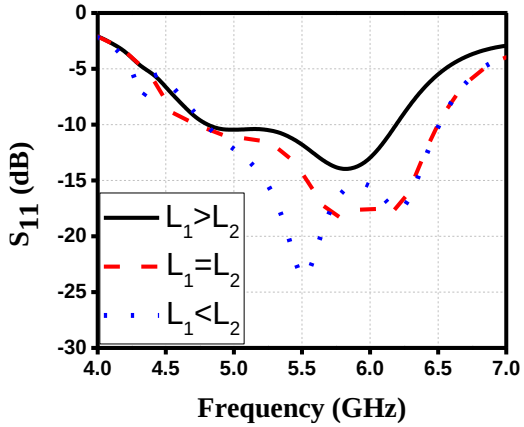

Fig. 6. Simulated reflection coefficient of the antenna with $L_1>L_2$, $L_1=L_2$ and $L_1<L_2$.

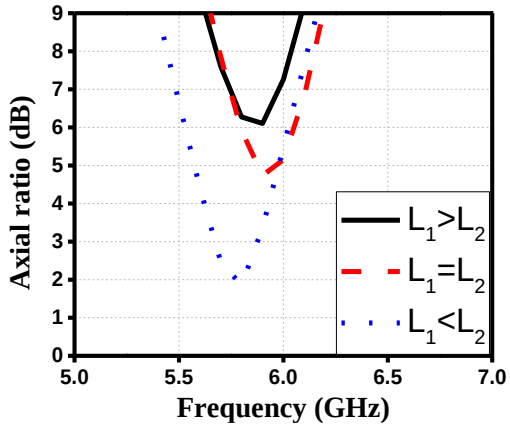

Fig. 7. Simulated axial ratio of the antenna when $L_1>L_2$, $L_1=L_2$ and $L_1<L_2$.

The minimum AR improves when $L_1<L_2$ with a 3-dB bandwidth of 3.47% (5.67–5.87 GHz) and a minimum AR value of about 2 dB at 5.75 GHz.

III. FABRICATION AND MEASUREMENT RESULTS

Using the annular slot and the X-shaped slotted circular patch etched on the bottom face of a superstrate, two superposed layers were assembled, and a prototype was fabricated as shown in Fig. 8. The antenna prototype was measured in a standard anechoic chamber. Foam is used for maintaining the air space between the two layers. An optimum gap height of H_c = 3.5 mm, which is $\lambda/15$ at 5.8 GHz, is verified experimentally. The reflection coefficient (S_{11}) is measured using an Agilent Vector Network Analyzer (VNA) 8722ES. Figure 9 shows the simulated and measured reflection coefficients of the proposed CP antenna. Simulated results show that the reflection coefficient is below -10 dB within the frequency range from 4.8 GHz to 6.5 GHz with an

impedance bandwidth of 1.7 GHz, which is about 30%. The impedance bandwidth of the fabricated CP antenna is 2 GHz from 4.5 GHz to 6.5 GHz, which is about 36%. It can be observed that a measured wideband reflection coefficient is achieved. The measured impedance bandwidth agrees with the simulated one. In addition, the trivial discrepancy between the simulation and measurement results is attributed to the unavoidable fabrication tolerance.

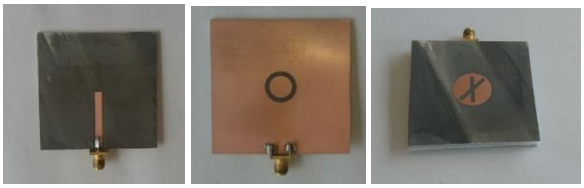

(a) (b) (c)

Fig. 8. Photograph of the fabricated prototype: (a) top view of the feeding annular slot, (b) microstrip feed line, and (c) bottom view of the X-shaped slot.

The simulated and measured AR are shown in Fig. 10. It can be seen that the measured AR has a lowest value of 1.6 dB at 5.8 GHz and 3-dB AR bandwidth of 3.47% form 5.67 GHz to 5.87 GHz. The lowest value of the simulated AR is about 1.83 dB at 5.8 GHz that supports WLAN bands. The 3-dB AR simulated bandwidth is still located within the impedance bandwidth of the proposed antenna and agrees well with the measured one.

Figure 11 shows the simulated and measured gain of the proposed CP antenna. It is illustrated that the simulated 3-dB gain bandwidth is about 46.62% (4.08-6.56 GHz), with a maximum gain of 8.85 dBi. The measured 1-dB gain bandwidth is about 19.5% from 4.85 GHz to 5.90 GHz. The maximum measured gain is about 8.65 dBi. The common bandwidth for measured 10-dB impedance and 1-dB gain is about 19.5% (4.85-5.90 GHz). It is worth mentioning that the measured gain is quite uniform with frequency over the operating bandwidth and agrees well with the simulated results.

Figure 12 shows the simulated and measured radiation patterns for both right-hand CP (RHCP) and left-hand CP (LHCP) at 5.8 GHz for phi=0° and phi=90° planes. It can be observed that the RHCP is radiated in the +Z direction, whilst LHCP in the -Z direction. In addition, the trivial discrepancy between the simulated and measured radiation patterns is attributed to the unavoidable fabrication tolerance and the presence of noise during the far-field measurement.

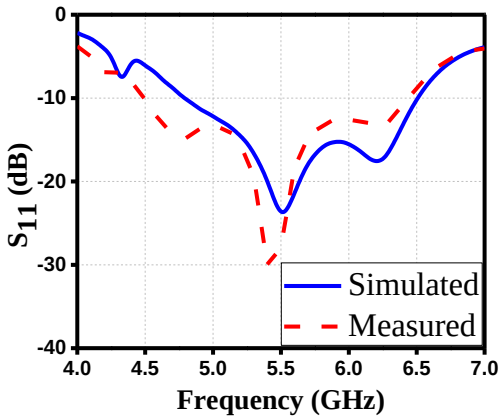

Fig. 9. Simulated and measured reflection coefficient of the proposed antenna.

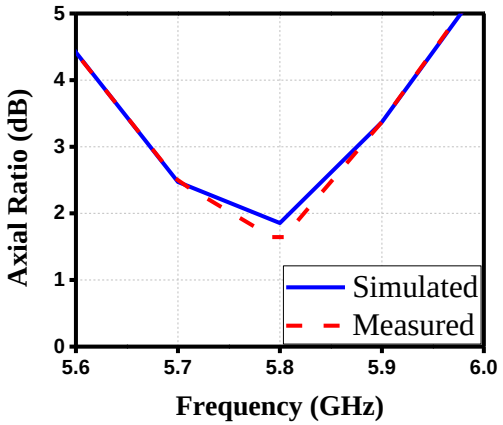

Fig. 10. Simulated and measured axial ratio of the proposed antenna.

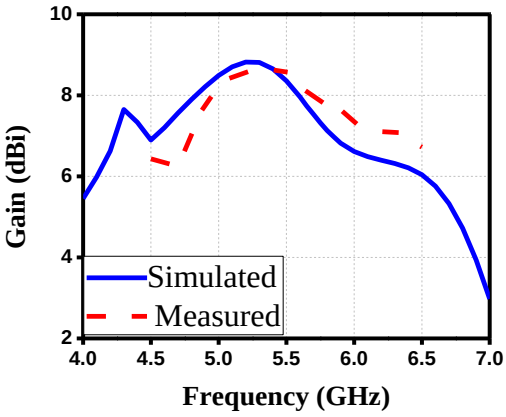

Fig. 11. Simulated and measured Gain of the proposed antenna.

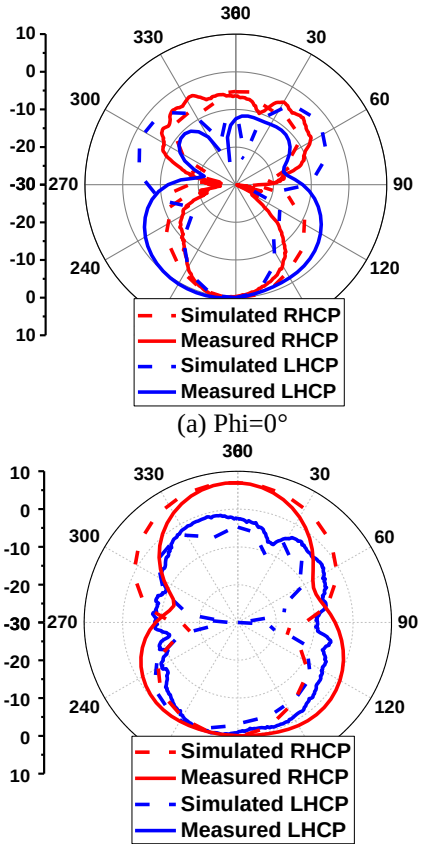

(a) Phi=0°

(b) Phi=90°

Fig. 12. Simulated and measured radiation patterns of the proposed antenna at 5.8 GHz at: (a) Phi= 0° and (b) Phi= 90°.

Table 2 presents a comparison of the proposed antenna with some previously published designs. As can be seen, the novel compact aperture-coupled CP antenna presented in this work has a better performance in terms of gain and 3-dB AR bandwidth compared with the published designs.

IV. CONCLUSION

A novel high gain compact aperture-coupled circularly polarized antenna for WLAN applications has been presented. The reported results have demonstrated that the circular polarization is obtained by employing the asymmetric X-shaped slot with an angle θ = 45° between the two arms etched on a circular patch antenna. Furthermore, the air gap between the X-shaped slot antenna substrate and the annular slot feeding substrate was used to maintain the gain of the proposed antenna. Consequently, the measured 1-dB gain bandwidth of 19.5% (4.85-5.90 GHz) and 3-dB AR bandwidth of 3.47% (5.67-5.87 GHz) are well overlapped by the measured 10-dB impedance bandwidth of 36% (4.5-6.5 GHz). The antenna has a maximum gain of 8.65 dBi. Measured results confirm that there is a good agreement between simulations and measurements.

ACKNOWLEDGMENT

This work was supported by King Fahd University of Petroleum and Minerals (KFUPM), Saudi Arabia, through DSR project No. GTEC1802 and by the Algerian Ministry of Higher Education and Scientific Research (MESRS). Authors would like to thank Mr. Arun Kesavan, EMT-INRS, for his help.

Table 2: Comparison of the proposed antenna with some previously published designs

Ref.	Size (mm^3)	Freq. (GHz)	S_{11} BW (%)	Gain Max	3-dB ARBW (GHz, %)
[16]	1.2 λ_0 × 1.2 λ_0 × 1.6	2.4/5.8	14.3/ 8.1	3.7/3.2 dBi	(≈5.7-5.93), 4.1
[22]	133.2 × 133.2 × 32.54	(2.37-2.75) (3.4–8)	14.84/80.70	5.95/6.92/6.37/6.07 dBic	5.7–5.87, 2.9
[23]	30 × 30 × 3.048	(2.43-2.52) (5.7-6.5)	3.63/13.11	6.6/6 dBi	(≈5.85-5.97), 2.03
Proposed antenna	60 × 60 × 5.83	(4.5-6.5)	36	7.8 dBi	5.67-5.87, 3.47

REFERENCES

[1] Y. Zhang, W. Yu, and W. Li, "Study on Fabry-Perot antennas using dipole exciters," *The Applied Computational Electromagnetics Society (ACES) Journal*, vol. 29, no. 12, pp. 1112-1115, Dec. 2014.

[2] M. A. Meriche, H. Attia, A. Messai, and T. A. Denidni, "Gain improvement of a wideband monopole antenna with novel artificial magnetic conductor," *17th International Symposium on Antenna Technology and Applied Electromagnetics (ANTEM)*, 2016.

[3] A. Chaabane, F. Djahli, H. Attia, L. M. Abdelghani, and T. A. Denidni, "Wideband and high-gain EBG resonator antenna based on dual layer PRS," *Microw. Opt. Technol. Lett*., vol. 59, no. 1, pp. 98-101, 2017.

[4] L. M. Abdelghani, H. Attia, and T. A. Denidni, "Dual and wideband Fabry–Perot resonator antenna for WLAN applications," *IEEE Antennas Wireless Propag. Lett.*, vol. 16, pp. 473-476, 2017.

[5] M. A. Meriche, A. Messai, H. Attia, B. Hammache, and T. A. Denidni, "High-gain wideband Fabry-Pérot slot antenna with partially reflective surface," *16th Mediterranean Microwave Symposium (MMS)*,

2016.

[6] Z. Jiang, H. Zhao, X. Zhao, J. Liu, M. Shui, T. Wan, and X. Qiao, "Gain-enhanced compact circularly polarized array microstrip antenna," *The Applied Computational Electromagnetics Society* (*ACES) Journal*, vol. 34, no. 3, pp. 397-402, Mar. 2019.

[7] M. A. El-Hassan, K. F. A. Hussein, A. E. Farahat, and K. H. Awadalla, "Shaped-beam circularly-polarized practical antenna array for land imaging SAR systems," *The Applied Computational Electromagnetics Society* (*ACES) Journal*, vol. 34, no. 5, pp. 642-653, May 2019.

[8] J. Su, Z. Li, Z. Li, Q. Guo, and Y. L. Yang, "Ku-band phase-gradient metasurface for broadband high-gain circularly polarized lens antenna," *The Applied Computational Electromagnetics Society* (*ACES) Journal*, vol. 34, no. 5, 2019.

[9] Nasimuddin, K. Esselle, and A. K. Verma, "High gain compact circularly polarized microstrip antenna," *TENCON 2005 - 2005 IEEE Region 10 Conference*, Melbourne, Qld., pp. 1-4, 2005.

[10] M. A. Choubar, S. Gupta, M. Farahani, A. R. Sebak, and T. A. Denidni, "Gain enhancement of circularly–polarized dielectric resonator antenna based on FSS superstrate for MMW applications," *IEEE Trans. Ant. Propag*., vol. 64, no. 12, pp. 5542-5546, 2016.

[11] K. Agarwal, Nasimuddin, and A. Alphones, "Triple-band compact circularly polarised stacked microstrip antenna over reactive impedance meta-surface for GPS applications," *IET. Microw. Ant. Propag.*, vol. 8, pp. 1057-1065, 2014.

[12] L. B. K. Bernard, Nasimuddin, and A. Alphones, "An E-shaped slotted-circular patch antenna for circularly polarized radiation and radiofrequency energy harvesting," *Microw. Opt. Technol. Lett*., vol. 58, no. 4, pp. 868-875, 2016.

[13] H. L. Zhu, S. Cheung, K. L. Chung, and T. I. Yuk, "Linear-to-circular polarization conversion using metasurface," *IEEE Trans. Ant. Propag.*, vol. 61, no. 9, pp. 4615-4623, 2013.

[14] J. K. Pakkathillam and M. Kanagasabai, "Circularly polarized broadband antenna deploying fractal slot geometry," *IEEE Antennas Wireless Propag. Lett*., vol. 14, pp. 1286-1289, 2015.

[15] N. Herscovici, Z. Sipus, and D. Bonefacic, "Circularly polarized single-fed wide-band micro-strip patch," *IEEE Trans. Ant. Propag*., vol. 51, no. 6, pp. 1277-1280, 2003.

[16] Y. Sung, "Dual-band circularly polarized pentagonal slot antenna," *IEEE Antennas Wireless Propag. Lett.*, vol. 10, pp. 259-261, 2011.

[17] Nasimuddin and Z. N. Chen. "Aperture-coupled asymmetrical C-shaped slot microstrip antenna for circular polarization," *IET. Microw. Ant. Propag.*, vol. 3, no. 3, pp. 372-378, 2009.

[18] J. S. Row, "Design of aperture-coupled annular-ring microstrip antennas for circular polarization," *IEEE Trans. Ant. Propag*., vol. 55, no. 5, pp. 1779-1794, 2005.

[19] T. F. Hung, J. Ch. Liu, Ch. Y. Wei, Ch. Ch. Chen, and Sh. Sh. Bor, "Dual-band circularly polarized aperture-coupled stack antenna with fractal patch for WLAN and WiMAX applications," *Int. J. RF. Microw. Compt. Aided. Eng*., vol. 24, no. 1, pp. 130-138, 2014.

[20] J. C. Liu, B. H. Zeng, L. Badjie, S. Drammeh, S. S. Bor, T. F. Hung, and D. Ch. Chang, "Single-feed circularly polarized aperture-coupled stack antenna with dual-mode square loop radiator," *IEEE Antennas Wireless Propag. Lett*., vol. 9, pp. 887-890, 2010.

[21] Y. T. Chen, S. W. Wu, and J. S. Row, "Broadband circularly-polarised slot antenna array," *Electron. Lett.*, vol. 43, no. 24, 2007.

[22] T. V. Hoang, T. T. Le, Q. Y. Li, and H. Ch. Park, "Quad-band circularly polarized antenna for 2.4/5.3/5.8-GHz WLAN and 3.5-GHz WiMAX applications," *IEEE Antennas Wireless Propag. Lett.*, vol. 15, pp. 1032-1035, 2016.

[23] S. Behera and D. Barad, "Circular polarized dual-band antenna for WLAN/Wi-MAX application," *Int. J. RF. Microw. Compt. Aided. Eng*., vol. 27, no. 1, pp. 1-7, 2017.